



Anti-inflammatory effect of lucidone in mice *via* inhibition of NF- κ B/MAP kinase pathway

K.J. Senthil Kumar, Han Wen Hsieh, Sheng-Yang Wang*

Core Laboratory of Plant Metabolomics in Biotechnology Centre, Department of Forestry, National Chung Hsing University, Kou Kung Road, Taichung 402, Taiwan

ARTICLE INFO

Article history:

Received 15 June 2009

Received in revised form 9 November 2009

Accepted 4 December 2009

Keywords:

Lucidone

Lindera erythrocarpa

Inducible nitric oxide synthase (iNOS)

Cyclooxygenase-2 (COX-2)

Nuclear factor- κ B (NF- κ B)

Adaptor protein-1 (AP-1)

ABSTRACT

Here, we investigated the anti-inflammatory activity of lucidone, a phytochemical isolated from the fruits of *Lindera erythrocarpa* Makino, against lipopolysaccharide (LPS)-induced acute systemic inflammation in mice. Male ICR mice were injected intraperitoneally with LPS (5 μ g/kg), and the effects of pretreatment with various concentrations of lucidone (50–200 mg/kg) for 12 h on the formation of nitric oxide (NO), prostaglandin-E₂ (PGE₂) and tumor necrosis factor (TNF- α) were analyzed. Lucidone inhibited the production of NO, PGE₂ and TNF- α production in LPS-induced mice, and also induced mRNA and protein levels of inducible nitric oxide synthase (iNOS), and cyclooxygenase-2 (COX-2). The two common response elements of the iNOS and COX-2 genes are nuclear factor- κ B (NF- κ B) and activator protein-1 (AP-1). NF- κ B nuclear translocation and DNA binding were inhibited by lucidone in the LPS-induced mice. Moreover, lucidone decreased the expression and phosphorylation of c-Jun N-terminal kinase (JNK) protein thereby causing the subsequent inhibition of AP-1 activity. Finally, our results indicated that lucidone was able to block mitogen-activated protein kinases activity and its downstream signaling activation of NF- κ B and AP-1. We thus conclude that lucidone exerts its anti-inflammatory effects in mice by inhibiting the expression of pro-inflammatory factors and their related signaling pathways.

© 2010 Elsevier B.V. All rights reserved.

1. Introduction

Inflammation is a central feature of many pathological conditions and is mediated by a variety of soluble factors and cellular signaling events. For example, NF- κ B-dependent gene expression plays an important role in inflammatory responses and increases the expression of gene encoding cytokines and receptors involved in pro-inflammatory enzymes such as iNOS and COX-2. In addition, ATF-2 a member of AP-1, an early transcription factor, is also involved in pro-inflammatory response either alone or by coupling with NF- κ B [1]. Under normal physiological conditions NF- κ B forms a complex with its inhibitors, I κ -Bs. Once I κ -Bs are phosphorylated, NF- κ B is released and translocated to the nucleus, where its target genes are then activated [2,3]. Two I κ -B kinases, IKK- α and IKK- β are involved in the

signal induced phosphorylation of I κ -Bs: I κ -B α degradation results in rapid changes in NF- κ B induction, whereas I κ -B β degradation is associated with prolonged NF- κ B activation [4,5]. NF- κ B activation mediates the expression of a number of rapid response genes involved in the inflammatory response to injury, including iNOS and COX-2 [4]. NF- κ B pathway is well characterized elsewhere, only a few studies have directly examined the alternative inflammatory signaling pathways such as the mitogen-activated protein kinase (MAPK) and extra cellular signal-regulated kinase 1 and 2 (ERK1/2) pathways [2,6]. MAPKs mediate inflammatory and mitogenic signals to activate transcription factors, particularly NF- κ B or AP-1. TNF- α is a multifunctional cytokine that plays key roles in acute and chronic inflammation, anti-tumor responses, and infection. AP-1, NF- κ B, iNOS, COX-2, TNF- α , and p38 MAPK have been exploited as molecular targets in drug discovery and development for inflammatory related diseases [7].

Lucidone is a naturally occurring cyclopentenone, which was initially isolated from the fruits of *Lindera lucida* (Lauraceae) [8,9] and subsequently from other species such as *Lindera erythrocarpa* [10,11]. Our recent *in vitro* studies suggest that lucidone inhibits LPS-induced inflammation in murine macrophage cells [11,12]. The present study demonstrates that lucidone exhibits its anti-inflammatory activity *via*

* Corresponding author. Department of Forestry, National Chung-Hsing University, 250 Kuo-Kuang Road, Taichung 402, Taiwan. Tel.: +886 4 22840345x138; fax: +886 4 22873628.

E-mail address: taiwanfir@dragon.nchu.edu.tw (S.-Y. Wang).

suppression of NF- κ B and AP-1 activity in LPS-induced *in vivo* acute systemic inflammation.

2. Materials and methods

2.1. Chemicals

Lucidone was prepared according to the protocol described previously [11]. Lucidone purity was above 99% according to high-performance liquid chromatography (HPLC) and ^1H NMR analysis. Lipopolysaccharide (LPS, *E. coli* 0127:138), curcumin (purity: 96%) and Griess reagent were purchased from Sigma-Aldrich (St. Louis, MO, USA). Rabbit polyclonal anti-iNOS and anti-COX-2 antibodies were purchased from Cayman Chemical (Ann Arbor, MI, USA). Rabbit polyclonal anti-NF- κ B p50 antibodies were purchased from Abcam (Cambridge, UK). Rabbit polyclonal anti- β -actin was purchased from Sigma-Aldrich. The Rabbit polyclonal anti-I κ -B α , anti-p-IKK- α , anti-NF- κ B p65, anti-MAPK and anti-phospho MAPK sampler kit was obtained from Cell Signaling Technology, Inc. (Danvers, MA, USA). All other chemicals and solvents used in this study were of the reagent grade or HPLC grade.

2.2. *In vivo* experiments

Animal treatment and tissue preparation were as described previously [13]. All animal experiments were conducted in accordance with the *Guide for the Care and Use of Laboratory Animals* and Taiwan laws relating to the protection of animals, and were approved by the local ethics committee. Four-week-old male ICR mice (Charles River, Taipei, Taiwan) weighing 30 ± 5 g were used for this study. Animals were housed in cages with food and water *ad libitum*. The light cycle was controlled automatically (12 h dark and 12 h light) and the room temperature was thermostatically regulated to $22 \text{ }^\circ\text{C} \pm 1 \text{ }^\circ\text{C}$. Prior to the experiments, animals were housed under these conditions for a week to become acclimatized. Mice were divided into 6 groups consisting of 5 mice each. Lucidone and curcumin were dissolved in saline which contain 2% DMSO, and administered to mice by intraperitoneal injection at various concentrations (lucidone, 50, 100 or 200 mg/kg, or curcumin, 100 mg/kg) 4 h before LPS injection (5 $\mu\text{g}/\text{kg}$). Control mice received vehicle (saline) only. Mice were sacrificed by decapitation during anesthesia with ethyl ether 12 h after LPS injection. Blood was collected in EDTA tubes and centrifuged at $500 \times g$ for 10 min at $4 \text{ }^\circ\text{C}$. Serum was obtained and stored at $-20 \text{ }^\circ\text{C}$. Heart, lungs, kidneys and liver were removed, frozen in liquid nitrogen and stored at $-80 \text{ }^\circ\text{C}$ until use.

2.3. Determination of nitric oxide production

The accumulated nitrite in the blood serum was measured as a colorimetric indicator of NO production based on the Griess reaction [14]. Briefly, 50 μl of blood serum and 50 μl of saline were mixed with an equal volume of Griess reagent, incubated at room temperature for 30 min, and then absorbed at 540 nm using an ELISA microplate reader (μ -Quant, BioTek Instruments, Winooski, VT, USA). For determination of nitrite from blood serum, reduction of nitrate to nitrite was performed under alkaline conditions prior to Griess assay [15]. Fresh serum and saline served as blanks in all experiments. The amount of nitrite in the samples was obtained by means of the NaNO_2 serial dilution standard curve and the nitrite production was quantified.

2.4. Determination of PGE_2 production

Fresh serum was collected from treated and control mice, centrifuged at $500 \times g$ for 10 min $4 \text{ }^\circ\text{C}$ and stored at $-80 \text{ }^\circ\text{C}$ until tested. The level of PGE_2 released into the blood serum was quantified using a specific Prostaglandin E_2 EIA Kit (Cayman Chemical) according to the manufacturer's instructions.

2.5. Determination of TNF- α production

The levels of TNF- α production were measured in blood serum diluted to a proper concentration using mouse TNF- α ELISA kit (Cayman Chemicals, Ann Arbor, USA) according to the manufacturer's recommendation. Serum was obtained and assayed for TNF- α production using the ELISA kit. Quantification was performed using ELISA reader.

2.6. Preparation of whole cell, cytosolic and nuclear extracts

Tissues were homogenized in liquid nitrogen using a pestle and mortar. Equal amounts of homogenated tissue were suspended in 1 ml of saline, centrifuged at $500 \times g$ for 5 min at $4 \text{ }^\circ\text{C}$. Mammalian Protein Extraction Reagent (Cayman Chemical) was used for the preparation of whole cell lysates following the manufacturer's instructions. Cytosolic and nuclear extraction was carried out using Nuclear and Cytoplasmic Extraction Reagents Kit No. 78833 (Pierce Biotechnology, Rockford, IL, USA). The protein concentration was determined using the Bio-Rad protein assay reagent according to the manufacturer's instructions.

2.7. Western blot analysis

Western blot analysis was performed as described previously [12]. Immunoblotting was performed with appropriate antibodies using the Enhanced Chemi-Luminescence (ECL) Western Blotting Reagent (Immobilon, Millipore, Billerica, MA, USA) and the image was visualized by a VL Chemi-Smart 3000 (Viogene Biotek, Sunnyvale, CA, USA) imaging device.

2.8. Electrophoretic mobility shift assay (EMSA)

EMSA was performed as described previously [16]. In brief, oligonucleotide probes: NF- κ B, forward primer 5'-ATG TGA GGG GAC TTT CCC AGG C-3', reverse primer 5'-GCC TGG GAA AGT CCC CTC ACA T-3'; AP-1, forward primer 5'-CGC TTG ATG AGT CAG CCG GAA-3', and reverse primer 5'-TTC CGG CTG ACT CAT CAA GCG-3' were synthesized by TRI Biotech (Taipei, Taiwan), and then annealed with TE buffer for 5 min at $94 \text{ }^\circ\text{C}$ and then gradually cooled for 3 h. Nuclear extract (20 $\mu\text{g}/\text{ml}$) was incubated with 20 ng of double-standard NF- κ B/AP-1 oligonucleotides for 30 min at room temperature along with 5 μl of binding buffer. The DNA protein complex was separated by 6% native polyacrylamide gel. Then the complex was visualized using Light-Shift Chemiluminescent EMSA Kit (Pierce Biotechnology), and luminescence intensity was quantitated by a VL Chemi-Smart 3000 (Viogene Biotek) imaging device.

2.9. RNA isolation and RT-PCR analysis

Total RNA was isolated from mouse liver tissue using Trizol Reagent according to the manufacturer's instructions (Invitrogen Life Technologies, Carlsbad, CA, USA). Quantitative real-time reverse-transcription polymerase chain reaction (RT-PCR) analysis for iNOS, COX-2 and G3PDH mRNA was performed using Applied Biosystems (AB) detection instruments and software. The AB system incorporates a gradient thermocycler and a 96-channel optical unit. For the quantitative analysis of mRNA expression, the AB system was employed using DNA binding dye, SYBR Green, for the detection of PCR products. The melting point, optimal conditions and the specificity of the reaction were first determined using a standard procedure. The working stock solution of SYBR Green was 1:100 (Bio-Rad). Quantitative PCR was carried out in a 48-well plate with 10 pmol forward and reverse primers, and the working solution SYBR green, using a PCR master mix, under the following conditions: $95 \text{ }^\circ\text{C}$ for 5 min, followed by 40 cycles at $95 \text{ }^\circ\text{C}$ for 1 min, $55 \text{ }^\circ\text{C}$ for 45 s and $72 \text{ }^\circ\text{C}$ for 30 s. G3PDH, a housekeeping gene, was chosen as an internal standard to control for variability in amplification because of differences in starting mRNA concentrations. The sequences of the PCR primers were as follows: iNOS, forward 5'-TCC TAC ACC ACA CCA AAC-3', reverse 5'-CTC CAA TCT CTG CCT ATC C-3';

COX-2, forward 5'-CCT CTG CGA TGC TCT TCC-3', reverse 5'-TCA CAC TTA TAC TGG TCA AAT CC-3'; G3PDH, forward 5'-TCA ACG GCA CAG TCA AGG-3', reverse 5'-ACT CCA CGA CAT ACT CAG C-3'. The copy number of each transcript was calculated as the relative copy number normalized by GAPDH copy number.

2.10. Determination of bioavailability and plasma levels of lucidone

Male ICR mice were used for this assay. Samples were obtained from five mice (weight, approximately 30 mg for each) at each time. Lucidone solution which was prepared in phosphate-buffered saline which contains 2% DMSO was administered by intraperitoneal injection. Mice were treated at the doses of 50, 100 and 200 mg of lucidone per kg of body weight. Blood samples were obtained at 2, 4, 8 and 12 h post dose by cardiac puncher from lightly ethyl ether-anesthetized mice. Blood drawn into 3 ml EDTA tube was centrifuged (500 ×g for 10 min at 4 °C) to isolate plasma. Lucidone concentration in plasma was analyzed by high-performance liquid chromatography (HPLC) by silica gel column (250 mm × 4.6 mm) eluted with *n*-hexane/ethyl acetate solvent system. Briefly, mice plasma (1 ml) was deproteinized with Trichloroacetic acid (TCA) and extracted with ethyl acetate (EA). A 3 ml of organic layer was evaporated and the dried residue was reconstituted with EA in the concentration of 10 mg/ml in *n*-hexane/ethyl acetate solvent. The injection volume was 20 µl. Separation was achieved on a 250 × 4.60 mm i.d., 5 µ particle size luna silica column (Peneonenex, Inc, Torrance, CA). The mobile phase was a gradient mixture of *n*-hexane. Analyses were carried out on an Agilent 1100 series chromatographic system which operated gradiently, at a flow-rate of 0.7 ml/min. Gradient elution was carried out at room temperature and UV detection was performed at 280 nm. The limit of quantification (LOQ) was 10 mg/ml. Recovery ranged between 54.2% and 56.7%. Regression of accuracy data yielded an overall mean recovery (55.4 ± 0.42%).

2.11. Statistical analysis

The results were expressed as the mean standard error of the mean for three independent experiments. The data were analyzed statistically by one-way ANOVA and different group means were compared by Duncan's multiple range tests. SPSS for Windows, version 10.0 (SPSS Inc. Chicago, IL, USA) was used for analysis of data. $P < 0.05$ was considered significant in all cases.

3. Results

3.1. Effect of lucidone on NO, PGE₂ and TNF-α production in LPS-induced mouse blood serum

To assess the effect of lucidone on LPS-induced NO production in mice blood serum, mice were treated with lucidone (50, 100, and 200 mg/kg) or curcumin (100 mg/kg) for 4 h then treated with LPS (5 µg/kg) for 12 h. Lucidone/curcumin and LPS were not added to the control group. Mice were sacrificed by decapitation during anesthesia with ethyl ether 12 h after LPS injection. Blood was collected in EDTA tubes and centrifuged at 500 ×g for 10 min at 4 °C. Serum was obtained and NO concentrations were measured using the Griess reaction. Lucidone was found to inhibit LPS-induced NO production in a concentration dependent manner with an average IC₅₀ of 51.1 mg/kg for three separate experiments (Fig. 1A). Lucidone also inhibited the LPS-induced increased production of the secreted forms of PGE₂ in the blood serum in a dose-dependent manner (Fig. 1B). PGE₂ production fell significantly from 158.2 pg/ml to 141.3 pg/ml and 119.4 pg/ml in the serum when treated with concentrations of 100 and 200 mg/ml of lucidone respectively. The TNF-α level in blood serum was increased to 141 ng/ml after LPS challenge. This value was significantly reduced by

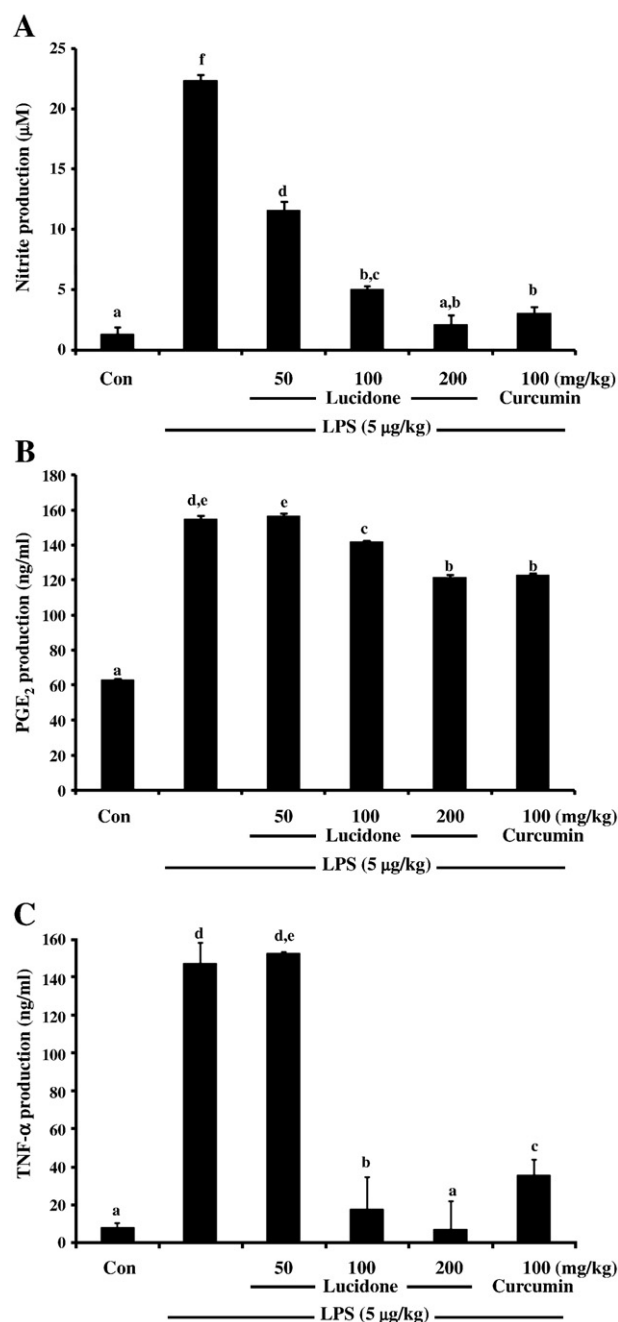


Fig. 1. Effects of lucidone on NO, PGE₂ and TNF-α production in LPS-induced mouse blood serum. Mice were treated with 5 µg/kg of LPS alone or LPS with the indicated concentrations of lucidone or curcumin for 12 h. Mice were sacrificed by decapitation 12 h after LPS injection. Blood was collected in EDTA tubes and centrifuged at 500 ×g for 10 min at 4 °C. Serum was obtained and NO (A); PGE₂ (B) and TNF-α (C) levels measured. Each value represents the mean ± S.E.M. of three independent experiments. Means not sharing a common letter were significantly different ($P < 0.05$) when analyzed by ANOVA and Duncan's multiple range test.

treatment with 100 and 200 mg/ml of lucidone to 17.90 and 8.20 ng/ml respectively (Fig. 1C).

3.2. Effects of lucidone on iNOS and COX-2 protein and mRNA expression in LPS-induced mouse liver tissue

The effects of lucidone on iNOS and COX-2 protein expression in heart, lung, kidney and liver of mice were determined after treatment with 50 mg/kg of lucidone for 4 h followed by challenge with 5 µg/kg LPS for 12 h. The highest iNOS expression was observed in lung followed

by liver [Fig. 1S(A)] and COX-2 expression was found in liver [Fig. 1S(B)]. We concluded that a major part of the LPS-induced inflammation in mouse model occurs in the liver. Moreover, the iNOS and COX-2 protein expression in liver tissue dramatically increased after LPS challenge. The increase in iNOS (Fig. 2A) and COX-2 (Fig. 2B) expression in liver was significantly reduced by pre-treatment with lucidone in a concentration dependent manner. Lucidone was found to significantly inhibit LPS-induced iNOS and COX-2 protein expression levels; we therefore reasoned that the inhibition could be due to suppression of iNOS and COX-2 at the transcriptional level. Interestingly, lucidone suppressed LPS-induced iNOS and COX-2 mRNA expressions in a dose-dependent manner (Fig. 2C and D). Curcumin, used as a reference compound in this study, was also an active inhibitor of iNOS and COX-2 protein as well as mRNA expression levels.

3.3. Effects of lucidone on nuclear translocation of NF- κ Bs and DNA binding activity in LPS-induced mouse liver tissue

To further investigate the mechanism of lucidone-mediated inhibition of iNOS and COX-2 transcription, we focused on NF- κ B, which is a known trans-active element of iNOS and COX-2 [17]. Here, initially, we presumed that lucidone inhibits the production of pro-inflammatory mediators *via* the NF- κ B pathway. To confirm if lucidone affects the

translocation of NF- κ B, we investigated the DNA binding activity of NF- κ B using EMSA. The results demonstrated that the DNA binding activity of NF- κ B was reduced in nuclear extracts obtained from LPS-activated mice liver tissue protein pretreated with lucidone and curcumin (Fig. 3). In addition, the localization of NF- κ B subunits, p65 and p50, in the nuclear extracts of mouse liver tissues were enhanced in the presence of LPS (5 μ g/kg) alone when compared with non-stimulated cells, whereas the localization of p65 (Fig. 4A) and p50 (Fig. 4B) was decreased in a dose-dependent manner with lucidone treatment. These results suggest that lucidone might interfere with the dissociation of I- κ B from the NF- κ B/I- κ B cytosolic complex, hence inhibiting nuclear translocation of NF- κ B.

3.4. Effects of lucidone on phosphorylation of IKK and I- κ B protein stability in LPS-induced mouse liver tissue

To examine whether lucidone inhibits LPS-induced phosphorylation of IKK and degradation of I- κ B, we prepared cytoplasmic extracts of mouse liver tissue and determined phosphorylation of IKK and I- κ B protein stability by Western blot. As shown in Fig. 5A, phosphorylation of IKK was notably inhibited by lucidone when compared with the negative control (treatment with LPS alone). I- κ B was degraded after treatment with LPS in mouse liver tissue for 12 h, and this degradation was markedly inhibited by pretreatment with lucidone in

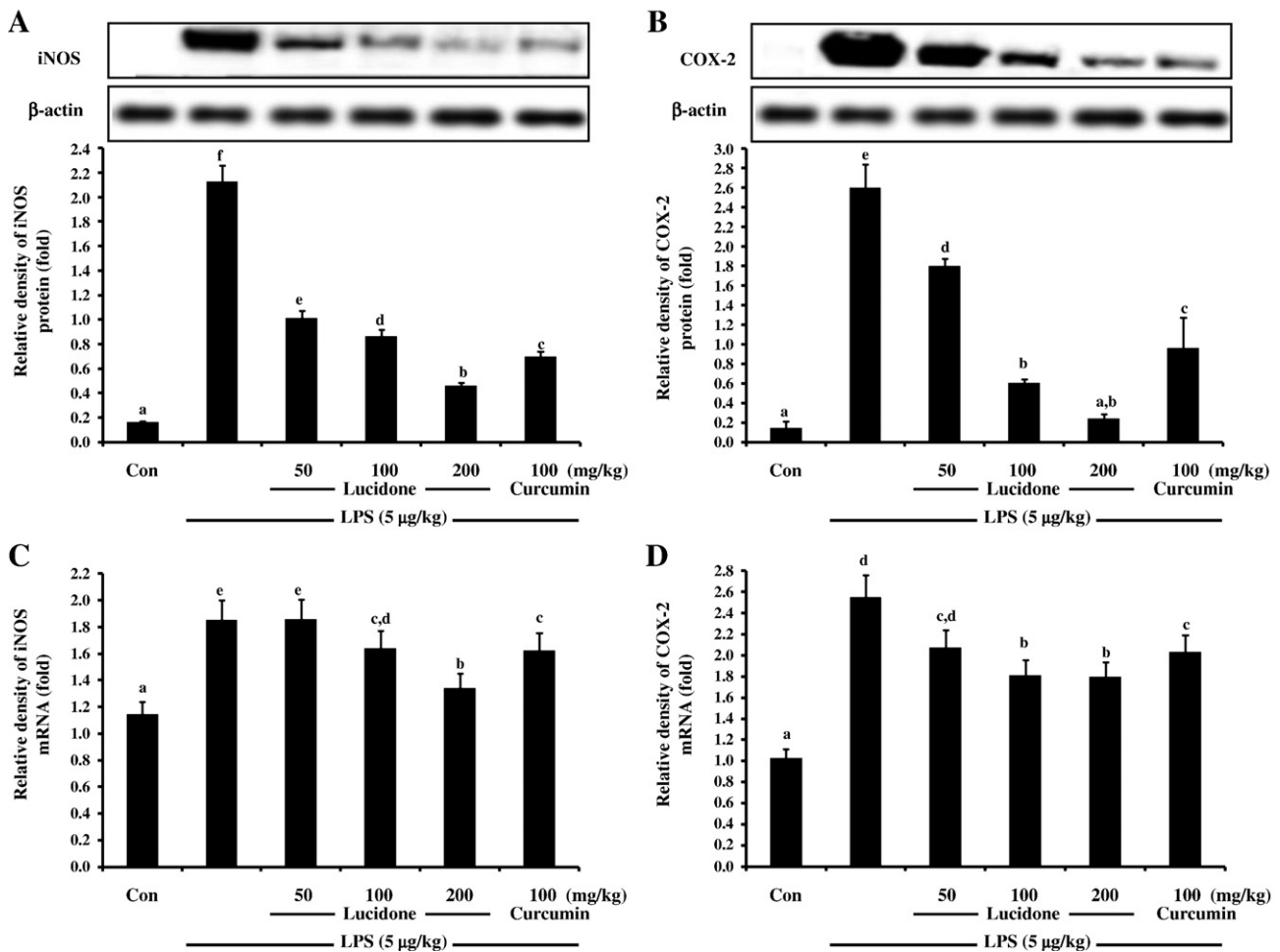


Fig. 2. Effect of lucidone on iNOS and COX-2 expression levels in LPS-induced mouse liver tissue. Mice were treated with 5 μ g/kg of LPS alone or LPS with indicated concentrations of lucidone and curcumin for 12 h. Mice were sacrificed by decapitation 12 h after LPS injection. Liver tissues were removed and homogenized. Total cell lysates were prepared and subjected to Western blot to analyze iNOS (A) and COX-2 (B) protein expression levels. In parallel, mice were treated with 5 μ g/kg of LPS or with the indicated concentrations of lucidone and curcumin for 8 h, and total RNA was subjected to RT-PCR. The RT products were labeled with SYBR Green dye. Relative iNOS (C) and COX-2 (D) mRNA expression ($2^{-\Delta\text{Ct}}$) was determined by RT-PCR and calculated by subtracting the Ct value for iNOS and COX-2 from G3PDH mRNA. $\Delta\text{Ct} = \text{Ct}_{\text{iNOS or COX-2}} - \text{Ct}_{\text{GAPDH}}$. Each value represents the mean \pm S.E.M. of three independent experiments. Means not sharing a common letter are significantly different ($P < 0.05$) when analyzed by ANOVA and Duncan's multiple range test.

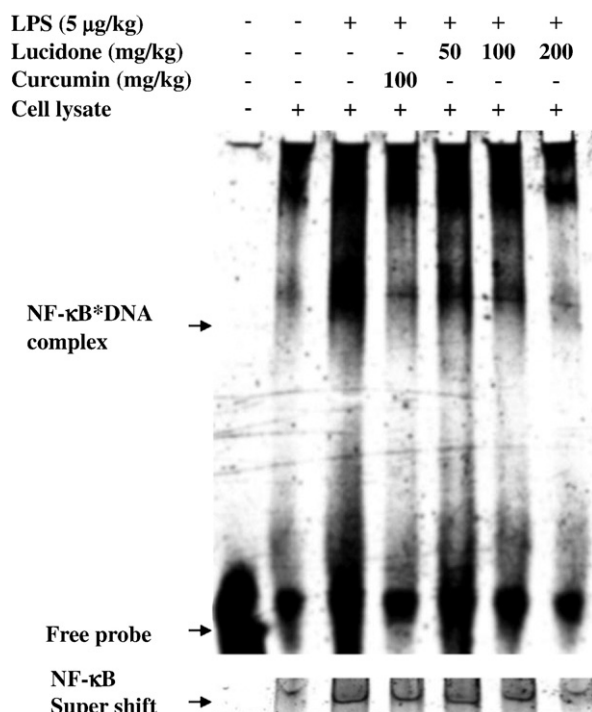


Fig. 3. Effect of lucidone on NF- κ B DNA binding activity in LPS-induced mouse liver tissue. Nuclear fractions were prepared from control mouse liver tissue, or from 12 h LPS (5 µg/kg)-stimulated mouse liver tissue with or without pretreatment with increasing concentrations of lucidone. Extracts were assayed for NF- κ B binding activity by EMSA as described in the Materials and methods section.

a dose-dependent manner (Fig. 5B). These results strongly suggest that lucidone inhibited the NF- κ B translocation to the nucleus through prevention of I- κ B α degradation.

3.5. Effects of lucidone on phosphorylation of JNK1/2 and p38 MAPK in LPS-induced mouse liver tissue

We examined the effect of lucidone on the phosphorylation of JNK1/2 and p38 MAPK in LPS-induced mouse liver tissue using Western blot analysis. As shown in Fig. 6, lucidone significantly inhibited LPS-induced activation of JNK1/2 and p38 MAPK in a concentration dependent manner. The amounts of non-phosphorylated JNK1/2 (Fig. 6A) and p38 MAPK (Fig. 6B) were unaffected by either LPS or lucidone treatment. Lucidone markedly inhibited JNK1/2 and p38 MAPK activation, while phosphorylation of ERK1/2 was unaffected by lucidone treatment (data not shown). These results indicate that MAPK phosphorylation was inhibited by lucidone pretreatment.

3.6. Effects of lucidone on AP-1 DNA binding ability in LPS-induced mouse liver tissue

The activation of MAPK cascade modulates AP-1 activation. We hypothesize that inhibition of MAPK signaling cascades by lucidone could be due to the poor ATF-2 activation and DNA binding ability of AP-1 through the nuclear translocation of phosphorylated MAPKs. Nuclear AP-1 DNA binding activity was significantly inhibited by lucidone, compared with non-stimulated cells and cells stimulated with LPS alone as shown in Fig. 7.

3.7. Effects of lucidone on nuclear translocation of phosphorylated MAPKs and activation of AP-1 in LPS-induced mouse liver tissue

We further evaluated the effects of lucidone on LPS-induced nuclear translocation of JNK1/2, p38 MAPK and activation of AP-1 in

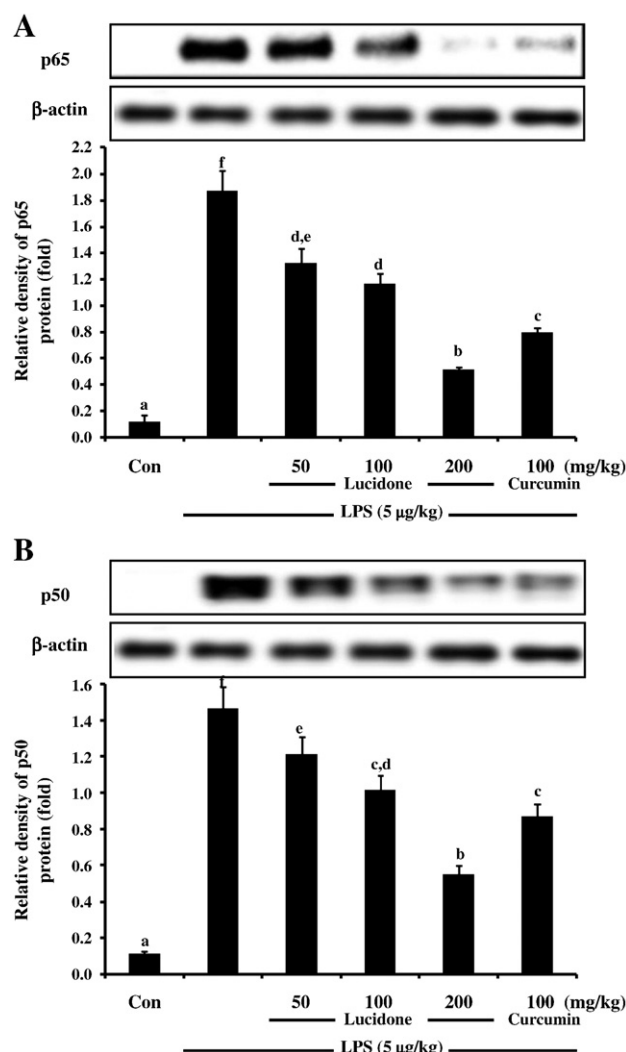


Fig. 4. Effect of lucidone on NF- κ B nuclear translocation in LPS-induced mouse liver tissue. Mice were treated with or without 5 µg/kg of LPS and with the indicated concentrations of lucidone or curcumin for 12 h, after which levels of p65 and p50 subunits of the NF- κ B in nuclear extracts were determined by Western blot. The histogram shows the relative intensity of p65 (A) and p50 (B) normalized to β -actin. Each value represents the mean \pm S.E.M. of three independent experiments. Means not sharing a common letter were significantly different ($P < 0.05$) when analyzed by ANOVA and Duncan's multiple range test.

LPS-induced mice. Lucidone significantly suppressed LPS-induced ATF-2 (part of the AP-1 complex) activity in a dose-dependent manner (Fig. 8A). These results suggest that lucidone inhibits the activation of ATF-2, which might be associated with the blocking of LPS-inducible iNOS and COX-2 expression. Since LPS-stimulated activation of ATF-2 is correlated with the translocation of phosphorylated JNK1/2 and p38 MAPKs, the effects of lucidone on phosphorylated JNK1/2 and p38 MAPK expression in the nuclear fraction was examined to clarify the inhibitory action of lucidone. Interestingly, lucidone attenuated phosphorylated JNK1/2 (Fig. 8B) and p38 MAPK (Fig. 8C) protein levels in the nuclear fraction. Taken together, these results suggest that lucidone inhibits both LPS-induced ATF-2 (AP-1) activation and phosphorylated JNK1/2 and p38 MAPK translocation.

3.8. Plasma concentration of lucidone

The concentration of lucidone in plasma after the intraperitoneal (i.p) injection with various concentrations of lucidone (50, 100 and

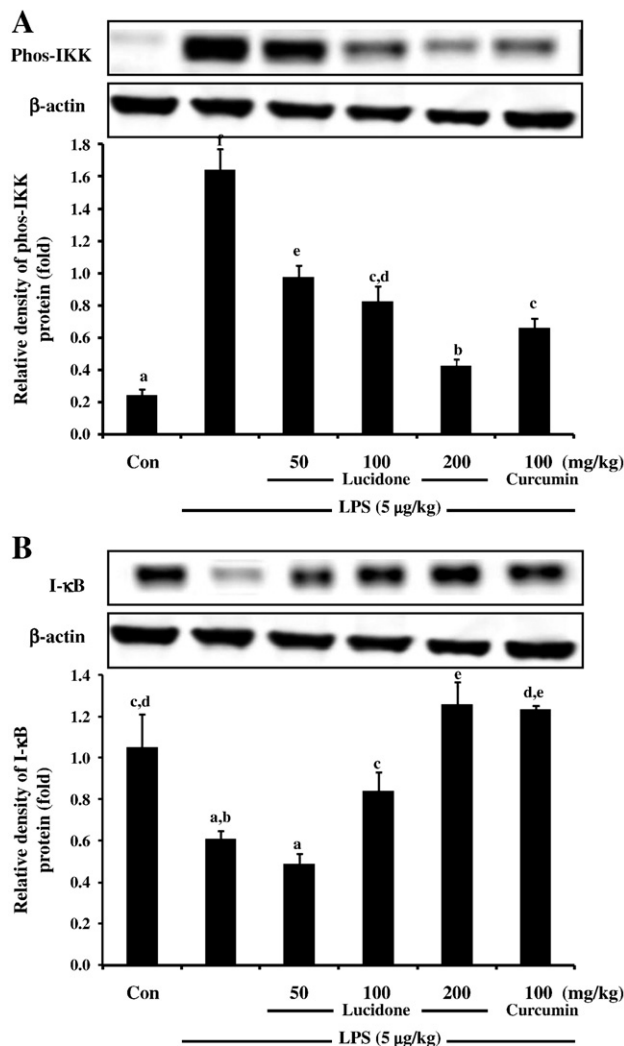


Fig. 5. Effects of lucidone on I-κB and phosphorylated IKK protein stability in LPS-induced mouse liver tissue. Mice were treated with or without 5 μg/kg of LPS and with the indicated concentrations of lucidone and curcumin for 12 h, when levels of I-κB and p-IKK in the cytoplasmic fraction were determined by Western blot. The histogram shows the relative intensity of I-κB (A) and p-IKK (B) normalized to β-actin. Each value represents the mean ± S.E.M. of three independent experiments. Means not sharing a common letter were significantly different ($P < 0.05$) when analyzed by ANOVA and Duncan's multiple range test.

200 mg/ml) for 12 h, either treated with single dose (200 mg/ml) with different time course (2, 4, 8 and 12 h) to mice were shown in Fig 2S(A) and (B). The plasma concentration of lucidone was increased after i.p administration of lucidone. It is clear from this figure that plasma level of lucidone was increased in relation to the dosing concentration [Fig 2S(A)]. Lucidone levels were below the LOQ of the analytical method at 12 h, in all animals. Maximum concentration of lucidone, after i.p injection, achieved at 4 h, was 368.5 μg/ml of plasma. The plasma concentration–time course of lucidone are shown in Fig 2S(B).

4. Discussion

Natural products have played a significant role in drug discovery and development, especially for diseases that have existed since antiquity. The present study was undertaken to elucidate the pharmacological and biological effects of lucidone isolated from the fruits of *L. erythrocarpa* Makino on the production of inflammatory mediators in a mouse model. Our previous studies demonstrated the anti-inflammatory mechanism

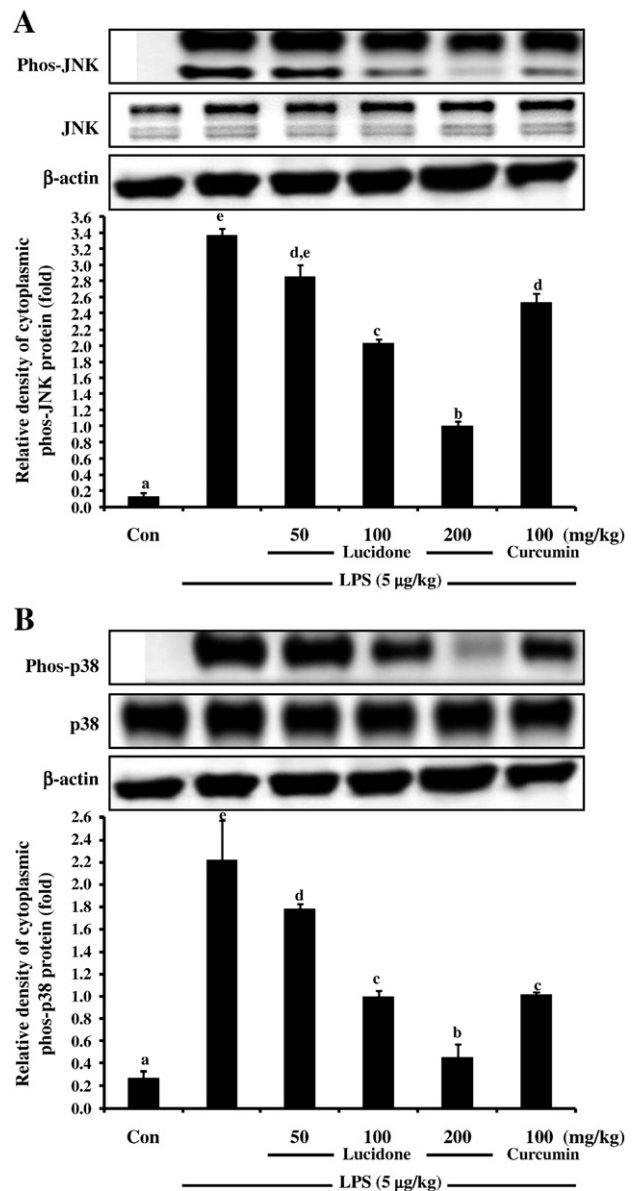


Fig. 6. Effect of lucidone on phosphorylation of MAPKs in LPS-induced mice liver tissues. Mice were treated with or without 5 μg/kg of LPS and with the indicated concentrations of lucidone and curcumin for 12 h. The phosphorylation of MAPKs was detected by immunoblotting using antibodies against the corresponding activated forms of MAPKs (phosphorylated MAPK). The histogram shows the relative intensity of p-JNK/JNK (A) and p-p38MAPK/p38MAPK (B) normalized to β-actin. Each value represents the mean ± S.E.M. of three independent experiments. Means not sharing a common letter were significantly different ($P < 0.05$) when analyzed by ANOVA and Duncan's multiple range test.

of lucidone under *in vitro* conditions using RAW 264.7 murine macrophage cells. Those results indicated that lucidone is an effective inhibitor of LPS-induced NO, PGE₂ and TNF-α production in RAW 264.7 cells and that its inhibitory effects are accompanied by a decrease in the expression of iNOS and COX-2 mRNA, and protein levels in a concentration dependent manner [11,12]. This suppression occurred in parallel with a decrease in the association of MAPK, I-κB/NF-κB and AP-1 activation [11,12].

Nitric oxide is recognized as a mediator and regulator of inflammatory response. NO is a free radical that is synthesized from *L*-arginine and is centrally involved in inflammation [18]. The production of TNF-α and NO is a crucial part of the immune response to some inflammatory stimuli. For example, excessive production of these mediators has been

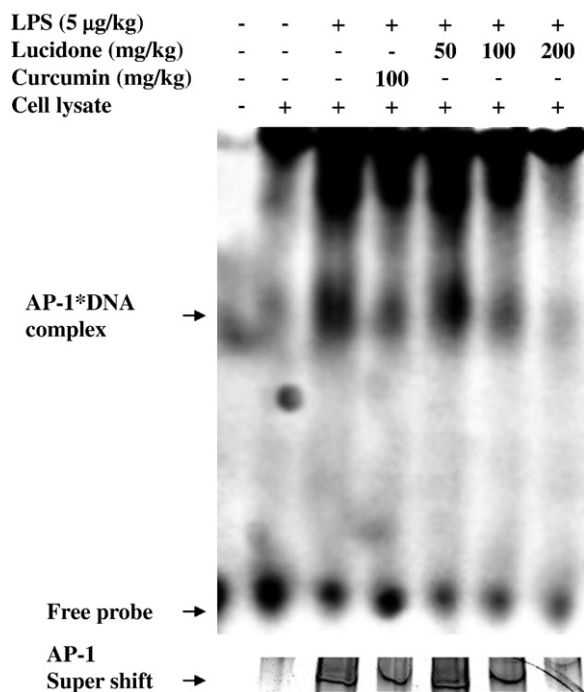


Fig. 7. Effect of lucidone on AP-1 DNA binding activity in LPS-induced mouse liver tissues. Mice were treated with or without 5 µg/kg of LPS and with the indicated concentrations of lucidone and curcumin for 12 h. The nuclear extract was incubated with AP-1 probes, and DNA binding was determined by EMSA assay as described in the Materials and methods section.

detected in septic and hemorrhagic shock, rheumatoid arthritis, and arthrosclerosis [19]. Thus, drug designs that decrease NO production by inhibiting the iNOS gene, major receptors for signaling initiated by LPS, or enzyme activity, have a therapeutic effect in the treatment of septic shock, as well as other many inflammatory and infectious disorders [20]. Furthermore, there are many reports of non-steroidal anti-inflammatory drugs inhibiting the production of NO and iNOS by the suppression of NF-κB activation [21].

In the present study, we evaluated the *in vivo* anti-inflammatory activity of lucidone in comparison to curcumin with regard to its ability to reduce the production of pro-inflammatory mediators. Intraperitoneal injection of LPS was used as a model of acute systemic inflammation. Our *in vivo* data strongly suggest that attenuation of the induction of cytokines such as TNF-α and the subsequent induction of NO formation in response to LPS, might in part, account for the clinical efficacy of cyclopentane in the treatment of inflammatory diseases. Accordingly, inhibition of cytokine formation may therefore affect the subsequent induction of this enzyme. On this account, we also investigated the effects of lucidone on iNOS and COX-2 expression. Pretreatment with lucidone inhibited the expression of iNOS and COX-2 in a concentration dependent manner. iNOS and COX-2 gene expression are regulated mainly at the transcriptional level in macrophages and their major transcriptional regulators are the NF-κB/AP-1 family of transcription factors, which are also key regulators of a variety of genes involved in immune and inflammatory responses [22]. The promoter of the iNOS and COX-2 gene is known to contain two transcriptional regions, an enhancer and a basal promoter [23]. There are a number of binding sites for transcription factors located in both the enhancer and basal promoter [22]. Importantly, the NF-κB/AP-1 binding site has been identified on the murine iNOS and COX-2 promoters and plays a role in the LPS-mediated induction of iNOS and COX-2 in macrophages [24]. In un-stimulated cells, NF-κB is present in the cytosol and is linked to the inhibitory I-κB protein. The transcriptional activation of NF-κB results in nuclear translocation

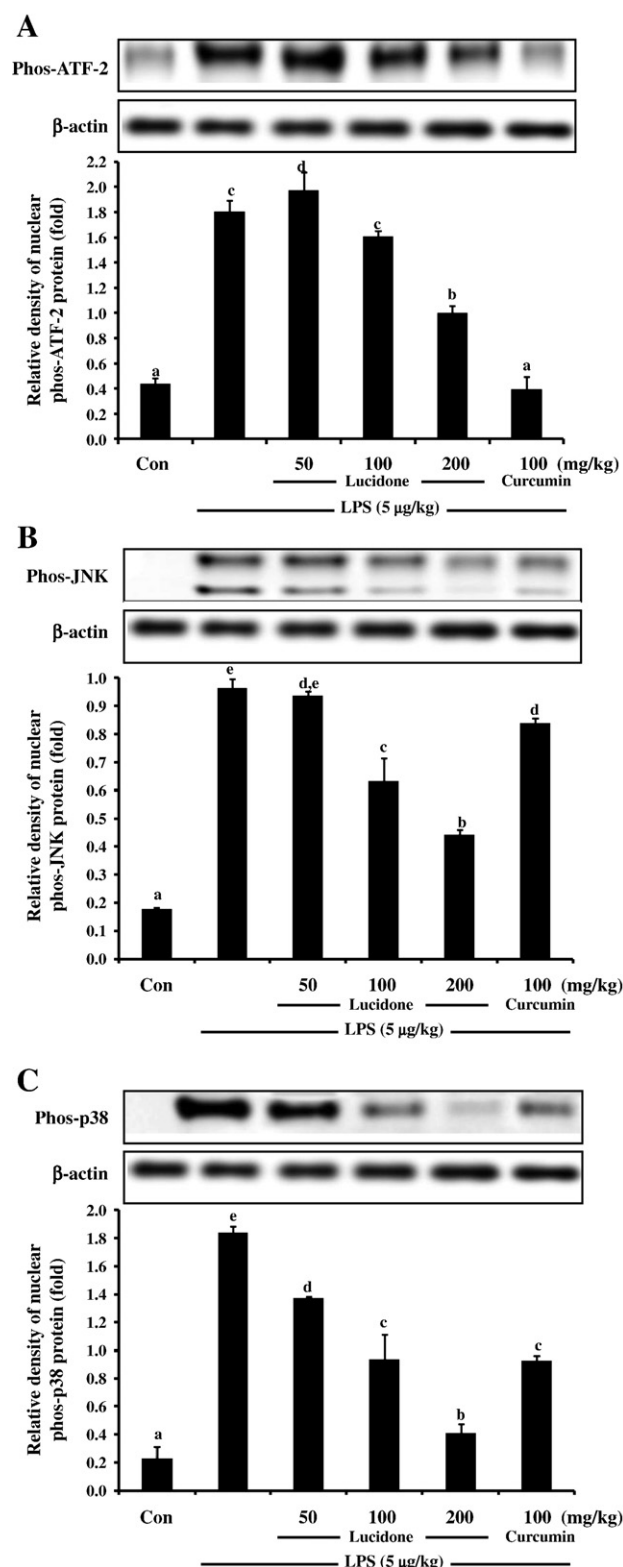


Fig. 8. Effect of lucidone on ATF-2 activation and MAPK translocation in LPS-induced mouse liver tissue. The levels of p-ATF-2, p-JNK and p-p38MAPK in the nuclear extract were determined by Western blot as described in the Materials and methods section. The histogram shows the relative intensity of p-ATF-2 and p-Elk-1 (A) p-JNK (B) and p-p38MAPK (C) normalized to β-actin. Each value represents the mean ± S.E.M. of three independent experiments. Means not sharing a common letter were significantly different ($P < 0.05$) when analyzed by ANOVA and Duncan's multiple range test.

and DNA binding ability, followed by phosphorylation, ubiquitination, and proteasome-mediated degradation of I- κ B proteins [25]. Our results indicate that lucidone inhibited the phosphorylation of IKK and cytosol I- κ B protein degradation. Moreover, lucidone inhibited nuclear translocation of NF- κ B and DNA binding ability in LPS-induced mouse liver tissue. Based on these results, we assume that the LPS-induced expressions of iNOS and COX-2 genes were inhibited by lucidone possibly through blocking NF- κ B activation. Based on the *in vivo* experiments, we ensure that lucidone plays a major role in the anti-inflammatory mechanism via the NF- κ B pathway.

However, only a few studies have directly examined the alternative inflammatory signaling pathways such as the MAPK and ERK1/2 pathways [2,6,23]. These MAPKs mediate inflammatory and mitogenic signals to activate transcription factors, particularly NF- κ B/or AP-1, thereby inducing a battery of pro-inflammatory genes [2,6]. Our previous reports have demonstrated an increase in AP-1 activity in response to LPS induction in macrophages, as well as a protective role for anti-inflammatory compounds, such as lucidone or curcumin, in the activation of pro-inflammatory factor production in LPS-induced murine macrophage cells [11,12].

In summary this study adds to the evidence that lucidone exerts inhibitory effects on LPS-induced pro-inflammatory cytokines, NO, TNF- α and PGE₂ production both *in vitro* and *in vivo*. This anti-inflammatory effect occurs by down-regulation of iNOS and COX-2 expression via the suppression of transcription factor NF- κ B activation and inhibition of I- κ B protein degradation in the pathophysiology of inflammatory disease. In view of the fact that NO and PGE₂ play important roles in mediating inflammatory responses, the inhibitory effects of lucidone on iNOS and COX-2 gene expression might be responsible for its anti-inflammatory action. In the future, further research is required to determine the anti-inflammatory properties of lucidone in human against inflammatory diseases such as bronchitis, inflammatory bowel disease (IBD), gastritis, and rheumatoid arthritis (RA).

Appendix A. Supplementary data

Supplementary data associated with this article can be found, in the online version, at doi:10.1016/j.intimp.2009.12.013.

References

- [1] Giuliani C, Napolitano G, Bucci I, Montani V, Monaco F. NF- κ B transcription factor: role in the pathogenesis of inflammatory, autoimmune, and neoplastic diseases and therapy implications. *Clin Ter* 2001;154:249–53.
- [2] Choi MS, Lee SH, Cho HS, Kim Y, Yun YP, Jung HY, et al. Inhibitory effect of obovatol on nitric oxide production and activation of NF- κ B/MAPK kinases in lipopolysaccharide-treated RAW 264.7 cells. *Eur J Pharmacol* 2007;556:181–9.
- [3] Israf DA, Khaizurin TA, Lajis NH, Khozirah S. Cardamonin inhibits COX-2 and iNOS expression via inhibition of p65NF- κ B nuclear translocation and I- κ B phosphorylation in RAW 264.7 macrophage cells. *Mol Immunology* 2007;44:673–9.
- [4] Tsai SH, Lin-Shiau SY, Lin JK. Suppression of nitric oxide synthase and the down-regulation of the activation of NF- κ B in macrophages by resveratrol. *Br J Pharmacol* 1999;126:673–80.
- [5] Kim BH, Cho SM, Reddy AM, Kim YS, Min KR, Kim Y. Down-regulatory effects of quercetin gallate on nuclear factor kappa B-dependent inducible nitric oxide synthase expression in lipopolysaccharide-stimulated macrophages RAW 264.7. *Biochem Pharmacol* 2005;69:1577–83.
- [6] Huh JE, Yim JH, Lee HK, Moon EY, Rhee DK, Pyo S. Prodigiosin isolated from *Hahella chejuensis* suppresses lipopolysaccharide-induced NO production by inhibiting p38 MAPK, JNK and NF- κ B activation in murine peritoneal macrophages. *Inter Immuno Pharmacol* 2007;7:1825–33.
- [7] Yang SY, Lambert JD, Hou Z, Ju J, Lu G, Hao X. Molecular targets for the cancer preventive activity of tea polyphenols. *Mol Carcinog* 2006;45:431–5.
- [8] Lee HH. The structure of lucidone and methyl lucidone. *Tetrahedron Lett* 1968;9:4243.
- [9] Leong YW, Harrison LJ, Bennett GJ, Kadir AA, Connolly JD. A dihydrochalcone from *Lindera lucida*. *Phytochem* 1997;47:891–4.
- [10] Oh HM, Chi SK, Lee JM, Lee SK, Kim HY, Han DC, et al. Cyclopentendiones inhibitors of farnesyl protein transferase and anti-tumor compounds, isolated from the fruits of *Lindera erythrocarpa* Makino. *Bioorg and Med Chem* 2005;13:6182–7.
- [11] Wang SY, Lan XY, Xiao J-H, Yang JC, Kao YT, Chang ST. Anti-inflammatory activity of *Lindera erythrocarpa* fruits. *Phytotherapy Res* 2008;22:213–6.
- [12] Senthil Kumar KJ, Wang SY. Lucidone inhibits iNOS and COX-2 expression in LPS-induced RAW 264.7 murine macrophage cells via NF- κ B and MAPKs signaling pathways. *Planta medica* 2009;75:494–500.
- [13] Lotter K, Hoehner K, Bucher M, Kees F. *In vivo* efficacy of telithromycin on cytokine and nitric oxide formation in lipopolysaccharide-induced acute systemic inflammation in mice. *J Antimicrob Chemother* 2006;58:615–21.
- [14] Miranda KM, Espey GM, Wink DA. A rapid, simple photometric method for simultaneous detection of nitrate and nitrite. *Nitric Oxide* 2001;5:62–71.
- [15] Green LD, Wagner DA, Glogowski J, Skippier PL, Wishnok JS, Tannenbaum ST. Analysis of nitrate, nitrite, and [¹⁵N] nitrate in biological fluids. *Anal Biochem* 1982;126:131–8.
- [16] Chiang YM, Lo CP, Chen YP, Wang SY, Yang NS, Kou YH, et al. Ethyl caffeate suppresses NF- κ B activation and its downstream inflammatory mediators, iNOS, COX-2, and PGE₂ *in vitro* or in mouse skin. *Br J Pharmacol* 2005;46:352–63.
- [17] Surh YJ, Chun KS, Cha HH, Han SS, Muhammad J, Zweifel BS, et al. Molecular mechanisms underlying chemopreventive activities of anti-inflammatory phytochemicals: down-regulation of COX-2 and iNOS through suppression of NF- κ B activation. *Mutat Res* 2001;480(1):243–68.
- [18] Choy CS, Hu CM, Chiu WT, Kei Lam CS, Ting Y, Tsai SH, et al. Suppression of lipopolysaccharide-induced of inducible nitric oxide synthase and cyclooxygenase-2 by Sanguis Draconis, a dragon's blood resin, in RAW 264.7 cells. *J Ethno Pharmacol* 2008;115:455–62.
- [19] Jarrar D, Kuebler JF, Rue LW, Matalon S, Wang P, Bland KI, et al. Alveolar macrophage activation after trauma-hemorrhage and sepsis is dependent on NF- κ B and MAPK/ERK mechanisms. *Amer J Physiol* 2002;283:L799–805.
- [20] Zang G, Ghosh S. Molecular mechanisms of NF- κ B activation induced by bacterial lipopolysaccharide through Toll-like receptors. *J Endotoxin Res* 2000;6:453–7.
- [21] Tanaka A, Hase S, Miyazawa T, Ohno R, Takeuchi K. Role of cyclooxygenase COX-1 and COX-2 inhibition in nonsteroidal anti-inflammatory drug-induced intestinal damage in rats: relation to various pathogenic events. *J Pharmacol Exptl Therapeutic* 2002;303:1248–54.
- [22] Xie QW, Kashiwabara Y, Nathan C. Role of transcription factor NF- κ B/Rel in induction of nitric oxide synthase. *J Biol Chem* 1994;269:4705–8.
- [23] Lowenstein CJ, Alley EW, Raval P, Snowman AM, Snyder SH, Russell SW, et al. Macrophage nitric oxide synthase gene: two upstream regions mediate induction by interferon gamma and lipopolysaccharide. *Proc Natl Acad Sci USA* 1993;90:9730–4.
- [24] Grandjean-Laquerriere A, Gangloff SC, Le Naour R, Trentesaux C, Hornebeck W, Guenounou M. Relative contribution of NF- κ B and AP-1 in the modulation by curcumin and pyrrolidine dithiocarbamate of the UVB-induced cytokine expression by keratinocytes. *Cytokine* 2002;18:168–77.
- [25] Park JS, Lee EJ, Lee JC, Kim WK, Kim HS. Anti-inflammatory effects of short chain fatty acids in IFN- γ -stimulated RAW 264.7 murine macrophage cells: Involvement of NF- κ B and ERK signaling pathways. *Inter Immuno Pharmacol* 2007;7:70–7.
- [26] Kundu JK, Surh YJ. Breaking the relay in deregulated cellular signal transduction as a rationale for chemo prevention with anti-inflammatory phytochemicals. *Mutation Res* 2005;591:123–46.